

[View the Full Text HTML](#)



## Dynamics of Low Temperature Induced Water Shedding from AOT Reverse Micelles

Alana K. Simorellis, Wade D. Van Horn, and Peter F. Flynn\*

Contribution from the Department of Chemistry, University of Utah,  
Salt Lake City, Utah, 84112-0850

Received October 13, 2005; E-mail: pfflynn@chem.utah.edu

**Abstract:** The effects of low temperature and ionic strength on water encapsulated within reverse micelles were investigated by solution NMR. Reverse micelles composed of AOT and pentane and solutions with varying concentrations of NaCl were studied at temperatures ranging from 20 °C to -30 °C. One-dimensional <sup>1</sup>H solution NMR spectroscopy was used to monitor the quantity and structure of encapsulated water. At low temperatures, e.g., -30 °C, reverse micelles lose water at rates that are dependent on the ionic strength of the aqueous nanopool. The final water loading ( $w_0 = [\text{water}]/[\text{surfactant}]$ ) of the reverse micelles is likewise dependent on the ionic strength of the aqueous phase. Remarkably, water resonance(s) at temperatures between -20 °C and -30 °C displayed fine structure indicating the presence of multiple transient water populations. Results of this study demonstrate that reverse micelles are an excellent vehicle for studies of confined water across a broad range of conditions, including the temperature range that provides access to the supercooled state.

### Introduction

Reverse micelles spontaneously form around an aqueous core upon the addition of certain surfactants to an apolar solvent and have applications in water confinement, biocatalysis, bioseparations, cosmetics, nanoparticle synthesis, and oil recovery.<sup>1-4</sup> According to the standard model of reverse micelle formation, nanoscale droplets of water promote the aggregation of the amphiphilic surfactant around a water core.<sup>5,6</sup> This water core is primarily defined by the water loading,  $w_0$ , which is defined as the molar ratio of water to surfactant. The radius of the reverse micelle naturally increases as a function of  $w_0$ , and several empirical relationships between  $w_0$  and the reverse micelle radius have been suggested.<sup>7</sup> At sufficient values of  $w_0$ , e.g.,  $w_0 > 10$ , reverse micelles are capable of solubilizing a variety of water soluble substances, including complex heteropolymers such as proteins and nucleic acids oligomers, as well as dyes of vastly different size and chemical composition.<sup>8</sup>

Water existing within living cells is frequently confined to nanoscale compartments, and its behavior under such circumstances has long been of interest. The results of studies from a number of disciplines suggest that water confined in such

clusters possesses physical properties that are distinct from that of bulk water.<sup>9-16</sup> A complete understanding of cellular systems thus depends on a solid understanding of the physical properties of confined water, and the water encapsulated within reverse micelles is of the proper dimension to serve as an effective model system for studies of cellular water.

Reverse micelles represent a flexible environment to study confined water across a relatively wide range of conditions. An important focus of previous studies has been the effects of the ionic strength on the physical properties of encapsulated water solutions, and a number of authors have investigated the effects of ionic strength on the uptake of water at ambient to high temperatures.<sup>17,18</sup> The maximum temperature of water solubilization has been reported to increase with increasing NaCl aqueous solution concentration, and the efficiency of water uptake is likewise influenced by both cation type and concentration.<sup>17,19</sup> Results of the current study complement previous investigations by charting the effect of ionic strength on reverse micelle stability at subzero temperatures and the accompanying phenomenon of water shedding, which is the loss of water content from a reverse micelle under perturbing conditions.<sup>20,21</sup>

- (1) Wand, A. J.; Babu, C. R.; Flynn, P. F.; Milton, M. J. In *Protein NMR for the Millennium*; Berliner, L. J., Ed.; Kluwer Academic/Plenum Publishers: New York, 2003; pp 121-160.
- (2) Nazário, L. M. M.; Crespo, J. P. S. G.; Holzwarth, J. F.; Hatton, T. A. *Langmuir* **2000**, *16*, 5892-5899.
- (3) Khmel'nitsky, Y. L.; Kabanov, A. V.; Klyachko, N. L.; Levashov, A. V.; Martinek, K. In *Structure and Reactivity in Reversed Micelles*; Pileni, M. P., Ed.; Elsevier: New York, 1989; p 230.
- (4) Robinson, B. H.; Khen-Lodi, A. N.; Tomey, T. In *Structure and Reactivity in Reversed Micelles*; Pileni, M. P., Ed.; Elsevier: Amsterdam, 1989; p 198.
- (5) Ueda, M.; Schelly, Z. A. *Langmuir* **1987**, *4*, 653-655.
- (6) Yu, Z. J.; Zhou, N. F.; Newman, R. D. *Langmuir* **1992**, *8*, 1885-1888.
- (7) Pileni, M. P. *J. Phys. Chem.* **1993**, *97*, 6961-6973.
- (8) Luisi, P. L.; Magid, L. J. *CRC Crit. Rev. Biochem.* **1986**, *20*, 409-474.
- (9) Salom, D.; Abad, C.; Braco, L. *Biochemistry* **1992**, *31*, 8072-8079.
- (10) Rariy, R. V.; Bec, N.; Saldana, J.-L.; Nametkin, S. N.; Mozhaev, V. V.; Klyachko, N. L.; Levashov, A. V.; Balny, C. *FEBS Lett.* **1995**, *364*, 98-100.
- (11) Anarbaev, R. O.; Elepov, I. B.; Lavrik, O. I. *Biochim. Biophys. Acta* **1998**, *1384*, 315-324.
- (12) Klyachko, N. L.; Levashov, P. A.; Levashov, A. V.; Balny, C. *Biochem. Biophys. Res.* **1999**, *254*, 685-688.
- (13) Gerhardt, N. I.; Dungan, S. R. *Biotechnol. Bioeng.* **2002**, *78*, 60-72.
- (14) Melo, E. P.; Costa, S. I. M. B.; Cabral, J. M. S.; Fojan, P.; Peterson, S. B. *Chem. Phys. Lipids* **2003**, *124*, 37-47.
- (15) Andrade, S. M.; Carvalho, T. I.; Viseu, M. I.; Costa, S. M. B. *Eur. J. Biochem.* **2004**, *271*, 734-744.
- (16) Levinger, N. E. *Nature* **2002**, *298*, 1722-1723.
- (17) Kon-No, K.; Kitahara, A. J. *Colloid Interface Sci.* **1970**, *33*, 124-132.
- (18) Kon-No, K.; Kitahara, A. J. *Colloid Interface Sci.* **1971**, *41*, 47-51.
- (19) Rabie, H. R.; Vera, J. H. *Fluid Phase Equilib.* **1996**, *122*, 169-186.

The influence on ionic strength at low temperatures reveals complex behavior, and the tuning of the ionic strength of reverse micelles for low-temperature experiments is a key development, making an important impact on the field of cryoenzymology and studies of supercooled water.

The average geometry of water hydrogen bonding networks in the reverse micelle is dependent on both the water loading and temperature.<sup>22,23</sup> The structure of encapsulated water is influenced by interactions with the surfactant headgroups (sulfonate in the case of AOT), dissolved ions, and the nanoscale dimensions of the reverse micelle interior. IR studies, at both low and ambient temperatures, suggest that reverse micelle water is less susceptible to phase transitions than bulk water, due to the specific structure of the hydrogen bond network of water within the reverse micelle, particularly at the interface.<sup>23,24</sup>

Relatively few investigations of reverse micelles have previously been conducted at lower temperatures, largely due to constraints imposed by limited reverse micelle stability.<sup>21,25,26</sup> Nevertheless, low-temperature encapsulation studies have been performed at temperatures as low as  $-100\text{ }^{\circ}\text{C}$ , which supports access to a supercooled state of water, e.g., liquid water cooled below the freezing point of pure water under standard laboratory conditions.<sup>21</sup> To access such a state with reverse micelles, it is necessary to limit the initial water loading; e.g., the initial water loading must be below 20.<sup>21,27</sup> The results of the current study will show that ionic strength is also capable of stabilizing the reverse micelles, allowing them to be cooled to below bulk water freezing temperatures with substantially increased flexibility in initial conditions. Studies of supercooled water have commonly been conducted under relatively demanding conditions, e.g., high pressure, or with the addition of other solutes. Water confined to small volumes, such as that generated using thin (1 mm) capillary tubes or in aerosols, can readily be supercooled since the smaller volume reduces homogeneous nucleation.<sup>28</sup> Reverse micelles likewise represent an effective alternative approach to studies of supercooled water.

The presence of multiple populations of reverse micelle encapsulated water has been suggested based on results obtained using differential scanning calorimetry (DSC) and fluorescence, IR, UV, and NMR spectroscopies.<sup>29–31</sup> Each technology brings strengths and liabilities, and a comprehensive understanding of the phenomenon depends on a careful consideration of data from several disciplines. Fluorescent and UV spectroscopies make use of probe molecules that report on the local environment, whereas IR and NMR spectroscopies employ a direct observation of changes in vibrational modes or the chemical shift,

respectively.<sup>32,33</sup> Analysis of far-IR data has identified distinct species of water encapsulated within reverse micelles on the basis of the OH stretching frequencies.<sup>34</sup> A complementary study using far-IR studies of the hindered rotational motion of encapsulated water also indicates the presence of multiple species.<sup>35</sup> Terahertz time-domain spectroscopy has also been used to characterize low-frequency modes, the character of which depends on the water content of the reverse micelles.<sup>36,37</sup> Low-temperature solution NMR studies presented here provide key evidence that confirms the existence of multiple populations of water.

## Experimental Materials and Methods

AOT (Dioctyl sulfosuccinate) was obtained from Sigma and used without additional purification. AOT is hygroscopic and was stored in a desiccator over  $\text{P}_2\text{O}_5$  to prevent the gradual uptake of water over time. *n*-Pentane- $d_{12}$  (98% D) was obtained from Cambridge Isotope Laboratories, Inc. and was used without further purification. Samples consisted of 0.1 M AOT in 650  $\mu\text{L}$  of deuterated pentane with a  $w_0$  of 20 (23.4  $\mu\text{L}$ ) of deionized 18 M $\Omega$  water or buffer. Buffers employed in this study were composed of 50 mM sodium acetate pH 5.0 with 0.25 M NaCl, 0.5 M NaCl, or 1 M NaCl. Due to the relative low boiling point of pentane solutions, e.g.,  $\sim 37\text{ }^{\circ}\text{C}$ , samples were studied using 5 mm OD septum-capped NMR sample tubes, which were purchased from Wilmad Glass.

All data were recorded on a Varian INOVA NMR spectrometer operating at 500 MHz  $^1\text{H}$ . A Varian 500 MHz 5 mm  $^1\text{H}$  PFG broadband indirect detection probe with an operational temperature range down to  $-100\text{ }^{\circ}\text{C}$  (P/N 993373-00) was employed for all experiments. Encapsulation dynamics were monitored using one-dimensional  $^1\text{H}$  NMR spectra recorded at 1 min intervals for a total measurement time of approximately 90 min. Temperature was calibrated using the method of Van Geet (Wilmad, P/N WGH-09).<sup>38</sup> Thermal equilibrium was established as follows. The system variable temperature was set at  $-30\text{ }^{\circ}\text{C}$ , and chemical shift differences between the  $^1\text{H}$  methyl and hydroxyl resonances in a sample of methanol were monitored as a function of temperature as per the method of van Geet. The method has been shown to be an accurate method of temperature calibration that obviates the need for thermocouple probes. The cooling system consisted of a dry  $\text{N}_2$  gas stream cooled to near the boiling point of  $\text{N}_2$  delivered at 15 LPM by passing a coil through a dewar filled with liquid  $\text{N}_2$ . The probe was pre-equilibrated to the experimental temperature. Under these circumstances the MeOH calibration sample reached the target temperature within 2–3 min. Note that the heat capacity for methanol is  $2.53\text{ J g}^{-1}\text{ mol}^{-1}$ , compared with pentane at  $2.32\text{ J g}^{-1}\text{ mol}^{-1}$ , and given that the samples have very similar volumes, the experimental temperatures are accurate as stated.<sup>39</sup> Proton chemical shifts were referenced relative to the AOT H1' resonance, which resonates at 3.2 ppm relative to TMS.<sup>40</sup>

All water loading values reported in this study were confirmed by direct measurements that are based on a comparison of the integral intensity of the water resonance(s) and the H1' resonance of AOT. In studies of confined water, the precise  $w_0$  employed is critical for accurate interpretation of the results and should always be directly evaluated,

- (20) Van Horn, W. D.; Simorellis, A. K.; Flynn, P. F. *J. Am. Chem. Soc.* **2005**, *127*, 13553–13560.
- (21) Munson, C. A.; Baker, G. A.; Baker, S. N.; Bright, F. V. *Langmuir* **2004**, *20*, 1551–1557.
- (22) Wong, M.; Thomas, J. K.; Nowak, T. *J. Am. Chem. Soc.* **1977**, *99*, 4730–4736.
- (23) Nucci, N. V.; Vanderkooi, J. M. *J. Phys. Chem. B* **2005**, *109*, 18301–18309.
- (24) Thompson, K. F.; Gierasch, L. M. *J. Am. Chem. Soc.* **1984**, *106*, 3648–3652.
- (25) Douzou, P.; Keh, E.; Balny, C. *Proc. Natl. Acad. Sci.* **1979**, *76*, 681–684.
- (26) Zulaf, M.; Eicke, H. F. *J. Phys. Chem.* **1979**, *83*, 480–486.
- (27) Balny, C.; Hui, B. H. G.; Douzou, P. *Jerusalem Symp. Quantum Chem. Biochem.* **1979**, *12*, 37–50.
- (28) Angell, C. A.; Shuppert, J.; Tucker, J. C. *J. Phys. Chem.* **1973**, *77*, 3092–3099.
- (29) Daum, U.; Wei, G.; Luisi, P. L. *Colloid Polym. Sci.* **1998**, *276*, 657–622.
- (30) Quist, P. O.; Halle, B. *J. Chem. Soc., Faraday Trans. 1* **1998**, *84*, 1033–1046.
- (31) Hauser, H.; Haering, G.; Pande, A.; Luisi, P. L. *J. Phys. Chem.* **1989**, *93*, 7869–7876.

- (32) Zhang, H. Z.; Bright, F. V. *J. Phys. Chem.* **1991**, *95*, 7900–7907.
- (33) Riter, R. E.; Willard, D. M.; Levinger, N. E. *J. Phys. Chem. B* **1998b**, *102*, 2705–2714.
- (34) Onori, G.; Santucci, A. *J. Phys. Chem.* **1993**, *97*, 5430–5434.
- (35) Venables, D. S.; Huang, K.; Schmuttenmaer, C. A. *J. Phys. Chem. B* **2001**, *105*, 9132–9138.
- (36) Boyd, J. E.; Briskman, A.; Colvin, V.; Mittleman, D. *Phys. Rev. Lett.* **2001**, *87*, 147401–147404.
- (37) Boyd, J. E.; Briskman, A.; Sayes, C. M.; Mittleman, D.; Colvin, V. *J. Phys. Chem. B* **2002**, *106*, 6346–6353.
- (38) Van Geet, A. L. *Anal. Chem.* **1970**, *42*, 679–680.
- (39) Lide, D. R., Ed. *CRC Handbook of Chemistry and Physics*, 79 ed.; CRC Press: Boca Raton, FL, 1998.
- (40) Ueno, M.; Kishimoto, H.; Kyogoku, Y. *Chem. Lett.* **1977**, 599–602.

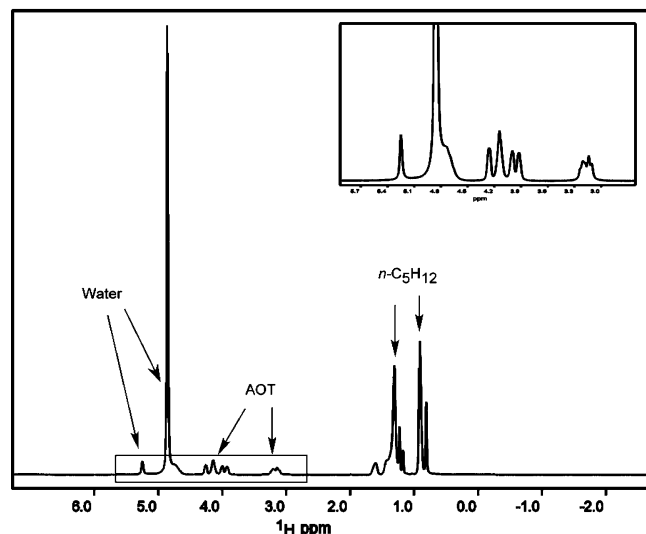


**Figure 1.** One-dimensional  $^1\text{H}$  spectrum of 0.1 M AOT and 0.5 M NaCl buffer at  $-20\text{ }^\circ\text{C}$ . The inset box expands the region of 3 ppm to 6 ppm that includes resonances from both water and AOT. Note the presence of multiple  $^1\text{H}$  water resonances, indicating multiple structural forms.

e.g., as opposed to estimates of  $w_0$  based on formulation.<sup>20</sup> Based on pilot experiments in which water resonance intensities and chemical shifts were monitored for intervals up to 3 h, an interval of 90 min was selected as the minimal length of time required to conduct a complete characterization of the time-dependent effects. No unexpected changes occurred during intervals longer than 90 min, and the conclusions of the study are unaltered by the inclusion of data from longer experiments.

## Results

The current investigation makes use of solution NMR methods to monitor the dynamics of encapsulated water at temperatures between  $20\text{ }^\circ\text{C}$  and  $-30\text{ }^\circ\text{C}$  at varying solution ionic strengths. Selection of NMR as the primary investigation method allows us to characterize the  $w_0$  directly over a wide range of temperatures, and through analysis of the  $^1\text{H}$  water resonance(s), we also gain insights into time-dependent changes in the structure of the encapsulated water, e.g., a dynamical perspective of the water shedding process. A representative  $^1\text{H}$  spectrum of buffer containing 0.5 M NaCl encapsulated within AOT reverse micelles, e.g., 0.1 M AOT/*n*-pentane, recorded at  $-20\text{ }^\circ\text{C}$  is shown in Figure 1. The intensity of the water resonance versus time for samples generated using buffers of increasing ionic strengths at temperatures from  $-30\text{ }^\circ\text{C}$  to  $20\text{ }^\circ\text{C}$  are shown in Figure 2. Results of these experiments confirm that the rate of temperature induced water shedding can vary substantially, depending upon the ionic strength and temperature of the encapsulated solution. The data in Figure 3 emphasizes the decrease of intensity of the water resonance as well as the upfield  $^1\text{H}$  chemical shift that occurs as  $w_0$  decreases. Reverse micelles composed of buffers of relatively low ionic strengths exhibit the most rapid loss of water, and in the limit of low ionic strength, e.g.,  $\text{d}_2\text{H}_2\text{O}$ , most of the encapsulated water is shed within the first 5 min of the experiment in both the  $-20\text{ }^\circ\text{C}$  and  $-30\text{ }^\circ\text{C}$  experiments, even before complete thermal equilibrium within the sample has occurred. Inspection of the low ionic strength samples after a 90 min exposure to low temperatures reveals the presence of ice at the bottom of the

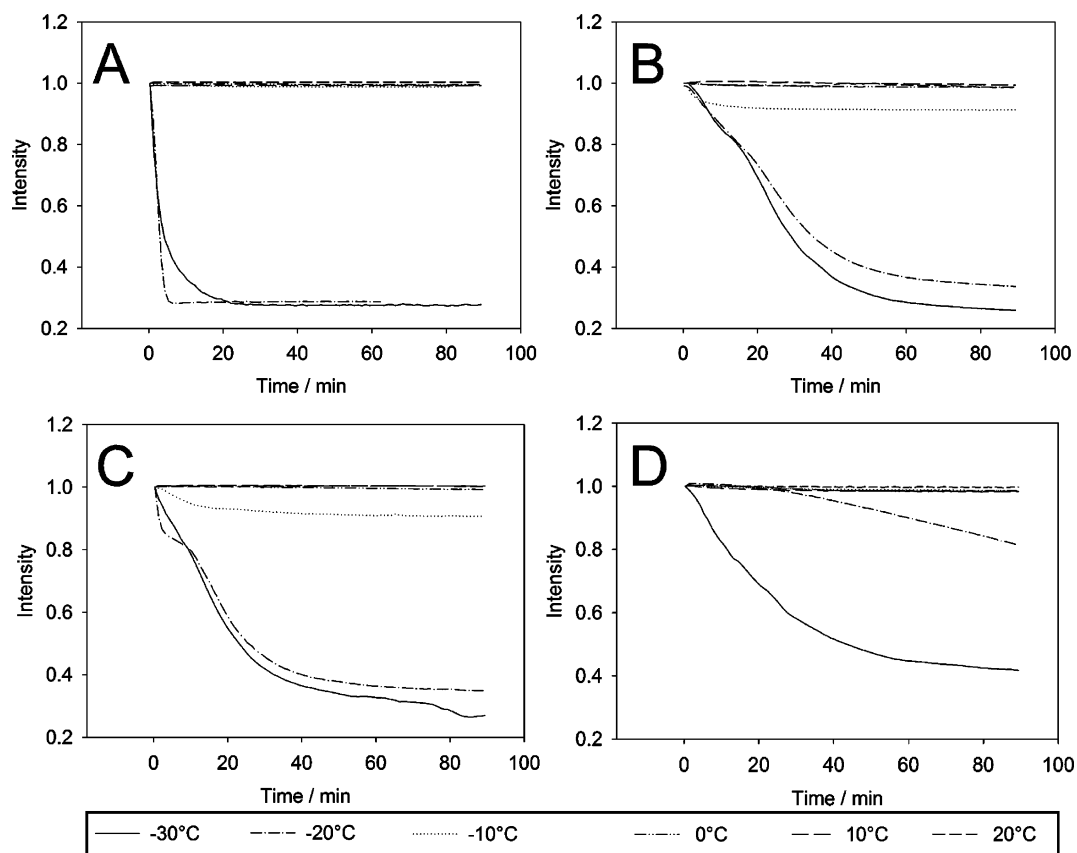


**Figure 2.** Normalized  $^1\text{H}$  water resonance intensity versus time at various temperatures. All samples were prepared to be 0.1 M AOT with a  $w_0$  of 20. Samples were prepared with (A)  $\text{d}_2\text{H}_2\text{O}$  or with (B) 0.25 M NaCl, (C) 0.5 M NaCl, or (D) 1 M NaCl. Plots chart the time-dependent loss of encapsulated water as a function of the solution ionic strength. Note that ionic strength affects both the rate of water shedding as well as the final  $w_0$ .

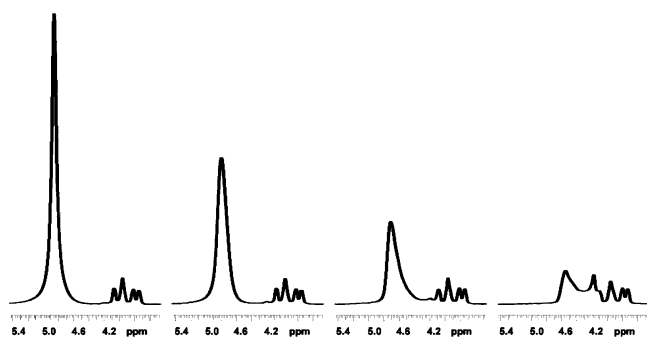


**Figure 3.** One-dimensional  $^1\text{H}$  spectrum of encapsulated ddH<sub>2</sub>O in AOT reverse micelles in *n*-pentane at  $-20\text{ }^\circ\text{C}$ . Spectra shown were recorded at 1 min intervals from the introduction of the sample into the probe and demonstrate the decreases in intensity, change in chemical shift, and broadening of the water resonance.

**Table 1.** Water Loading at  $-30\text{ }^\circ\text{C}^a$

ionic strength	$w_0(t=0)$	$w_0(t=\infty)$	$w_0(t_{1/2})$ (min)
dd(H <sub>2</sub> O)	44.4	0.240	4.0
0.25 M NaCl	29.3	5.78	29.0
0.50 M NaCl	26.7	7.49	23.0
1 M NaCl	22.7	8.41	43.0

<sup>a</sup>  $w_0(t=0)$  is initial water loading.  $w_0(t=\infty)$  is the intensity of the water resonance at infinity.  $w_0(t_{1/2})$  is the time it takes for the initial  $w_0$  to decrease to half its initial intensity. Two trends appear in the following table. Samples of low ionic strength have high  $w_0$  before the experiment and low  $w_0$  afterward. Samples of high ionic strength start with low  $w_0$  but have the highest  $w_0$  after the experiment. Sample temperature was established within 5 min of sample being introduced to the spectrometer. After 90 min, there were minimal changes in the system as monitored by resonance intensity and chemical shift changes.

NMR tube. After the sample is reequilibrated to room temperature, a biphasic water–pentane system forms, consistent with the experimentally observed  $w_0$  measurements that confirm water shedding.

Water shed from reverse micelles at low temperature was taken back up by the reverse micelles at a rate of about 1  $w_0$  unit per day if the sample is left unperturbed, whereas agitation of the sample reestablishes the original water loading within a few minutes.

Reverse micelles prepared using solutions of relatively high ionic strength, e.g., 50 mM sodium acetate, pH 5.0, and 1 M NaCl, produced the most stable low-temperature water nano-dispersions (see Table 1). For the sample mentioned above, the interval for the  $w_0$  to be reduced to half the initial  $w_0$  was approximately 40 min at  $-30\text{ }^\circ\text{C}$ . Note that since the change in intensity is clearly not a simple single exponential, we have deliberately avoided using the term “half-life”.

The sample containing ddH<sub>2</sub>O at  $20\text{ }^\circ\text{C}$  had the largest initial  $w_0$ , and at this temperature a constant volume of added water/buffer produces a  $w_0$  that steadily decreased as the salt concentration was increased, an effect which has been previously assumed.<sup>41</sup> Conversely, the sample with the highest ionic strength retained the highest  $w_0$  at  $-30\text{ }^\circ\text{C}$ . Although high ionic strength inhibits the minimum water loading capacity at room temperatures, at temperatures below zero, higher ionic strength facilitates greater water retention (see Figure 4). The size of AOT reverse micelles has been consistently shown to depend on water loading in a reliable manner.<sup>16,33,42</sup> In simplest terms,

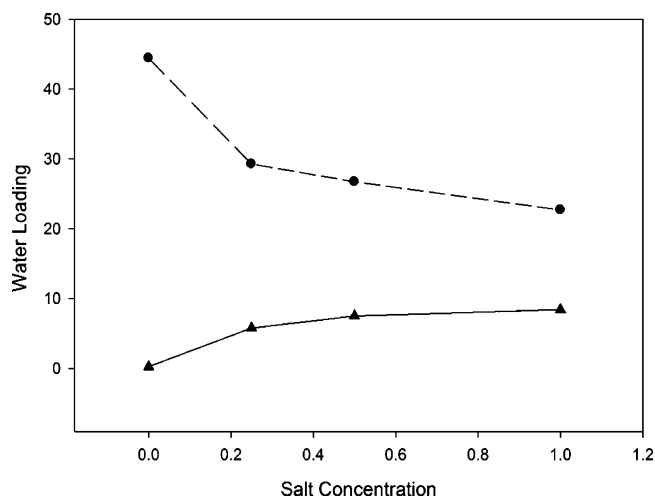


**Figure 4.** Water loading as a function of ionic strength. Circles indicate data recorded at  $20\text{ }^\circ\text{C}$ , and triangles specify data recorded at  $-30\text{ }^\circ\text{C}$ . As salt concentration increases at ambient temperature, the water loading capacity of reverse micelles decrease, whereas, at subzero temperatures, the micelles with the highest ionic strength have the largest water loading capacity.

as the ionic strength of the encapsulated solution is increased, reverse micelles shed water at slower rates and retain higher final  $w_0$  values.

Complex behavior of the  $^1\text{H}$  water resonance is manifest in data recorded at higher ionic strength and low temperature. Spectra recorded for samples containing 0.25 M, 0.5 M, and 1 M NaCl monitor not only a change in the chemical shift of the water resonance toward higher field but also the dynamic appearance of multiple water resonances (see Figures 5 and 6). Representative  $^1\text{H}$  spectra from the time series for a 0.5 M NaCl sample at  $-30\text{ }^\circ\text{C}$  are shown in Figure 5. This figure reveals multiple water resonances which vary in both intensity and chemical shift, and this fine structure reflects the presence of multiple populations of water that evolve during the course of the experiment.

The time-dependent changes in the  $^1\text{H}$  water chemical shifts reveal a general decrease in the chemical shift as a function of time, consistent with changes in hydrogen bonding present in the encapsulated water pools at room temperature (see Figures 3 and 6).<sup>22</sup> The chemical shift of the water resonance is primarily dependent upon the water loading. The water loading is in turn dependent upon the temperature and the concentration of salt in the solution used to prepare the sample. At room temperature, the samples with the lowest salt concentrations have the highest water loading, whereas this trend is reversed at low temperature. With respect to the chemical shift of the water resonance considered at low temperature, it should be noted that the structure of the supercooled water is anticipated to have a hydrogen bonding structure distinct from that of liquid water, leading to small chemical shift differences between the samples at the end of the experiment.

Bulklike encapsulated water within reverse micelles will sample multiple environments on a time scale of  $10^{-4}\text{ s}^{-1}$  at room temperature; the NMR experiment will measure this as a time averaged phenomenon.<sup>22</sup> However, samples prepared using solutions containing 50 mM sodium acetate pH 5.0 with 0.25 and 0.5 M NaCl at  $-20\text{ }^\circ\text{C}$ ,  $-30\text{ }^\circ\text{C}$ , and 1 M NaCl at  $-30\text{ }^\circ\text{C}$  (Figures 5 and 6) all show multiple coexisting water resonances. Bulk water represents relatively mobile water molecules that

(41) Kitahara, A.; Kon-No, K. *J. Phys. Chem.* **1966**, *70*, 3395–3398.

(42) Leser, M. E.; Luisi, P. L. *Chimia* **1990**, *44*, 270–282.

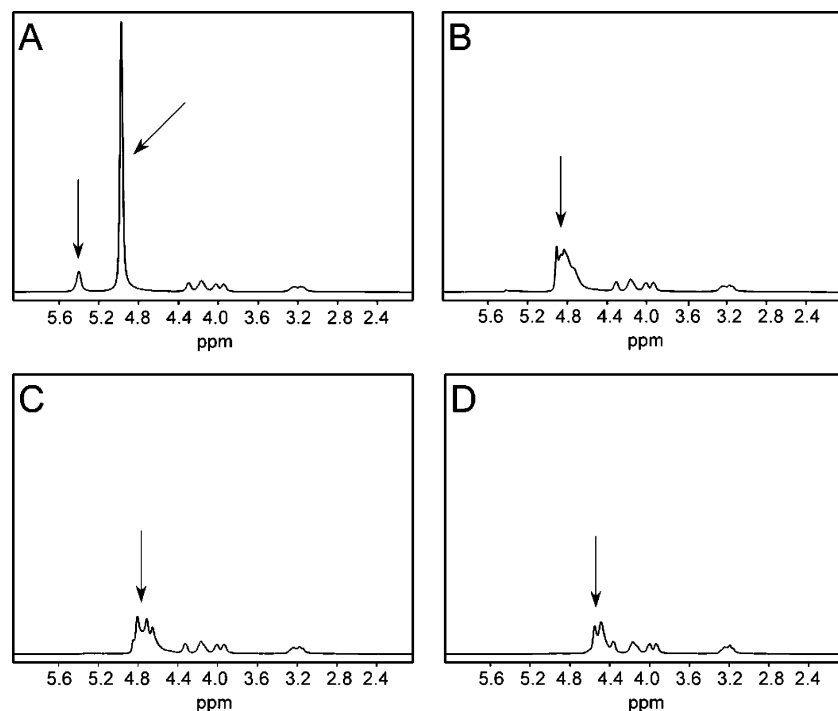


**Figure 5.** Time dependent intensity and chemical shifts of multiple  $^1\text{H}$  water resonances at  $-30\text{ }^\circ\text{C}$ . Arrows indicate either a single water resonance or an area with multiple water resonances. Note the time-dependent development of multiple water resonances. Sample was composed of 50 mM NaOAc, pH 5.0, 0.5 M NaCl. Selected spectra recorded at (A) 1 min, (B) 15 min, (C) 30 min, and (D) 40 min. Arrows in (A) indicate two separate resonances, (B) and (C) arrows indicate a triplet, and that in (D) indicates a doublet. The small downfield peak in (A) represents water solubilized in pentane at  $-30\text{ }^\circ\text{C}$ .

would be expected to sample multiple environments on the time scale of the measurement. As water is shed from the reverse micelle core, the number of mobile water molecules decreases and the relative proportion of water strongly associated in solvation of ions increases. Results of the current study indicate that a decrease in the rate of exchange between the waters of hydration of different ions is associated with the relative loss of bulk water. Although the rate of exchange between bulk water and water associated with less mobile forms has been estimated to occur on a time scale of  $10^{-4}\text{ s}^{-1}$ , our observations indicate that, at relatively high ionic strength and low temperatures, encapsulated water is restricted to distinct environments with residence times that persist on a much longer time scale (see Table 2).

The chemical shift of the water protons in water shifts downfield (deshielding) as hydrogen bonding geometry is optimized.<sup>22</sup> Results presented here show that the chemical shift of the encapsulated water  $^1\text{H}$  resonance is relatively sensitive to  $w_0$  changes and moves upfield with decreasing  $w_0$ . The interpretation of this effect is that, at low  $w_0$ , most of the water molecules contribute to solvation of the surfactant head-group at the expense of an optimal hydrogen bonding geometry. Also, the visualization of multiple water resonances verifies the existence of multiple water structures within the reverse micelles. At low temperatures, water is lost from the reverse micelle forcing the remaining water molecules to adopt different geometries, and these geometries can be manifest themselves as resonances at a particular chemical shift. Certain geometries are found in both 500 mM and 250 mM NaCl. Note the green line at 4.8 ppm at  $-30\text{ }^\circ\text{C}$  as well as the purple and blue lines at 4.6 at  $-30\text{ }^\circ\text{C}$ . Conversely, any additional water molecules made available through higher water loading supports

an average hydrogen bonding geometry that results in an averaged downfield shift of the water resonance (see Discussion section).

The main encapsulated water resonance occurs at a chemical shift of 4.8–5.0 ppm. The main water resonance exhibits rather complex time-dependent changes and shifts upfield as a function of time with  $w_0$ . Fine structure components of the water resonance appear after approximately 20 min at  $-20$  and  $-30\text{ }^\circ\text{C}$ , which further develop as water shedding proceeds.

A minor low-field component is also present at a  $^1\text{H}$  chemical shift of  $\sim 5.3$  ppm (see Figure 6). This resonance was unambiguously assigned to supercooled water in pentane by recording a  $^1\text{H}$  reference spectrum of  $\text{ddH}_2\text{O}$ -saturated *n*-pentane at  $-30\text{ }^\circ\text{C}$ . This water resonance appears precisely at the same position of the minor low-field  $^1\text{H}$  resonance observed in the reverse micelle spectrum, and its intensity decreases at the same rate as that resonance, confirming the identity of that resonance as supercooled water in *n*-pentane.

## Discussion and Conclusions

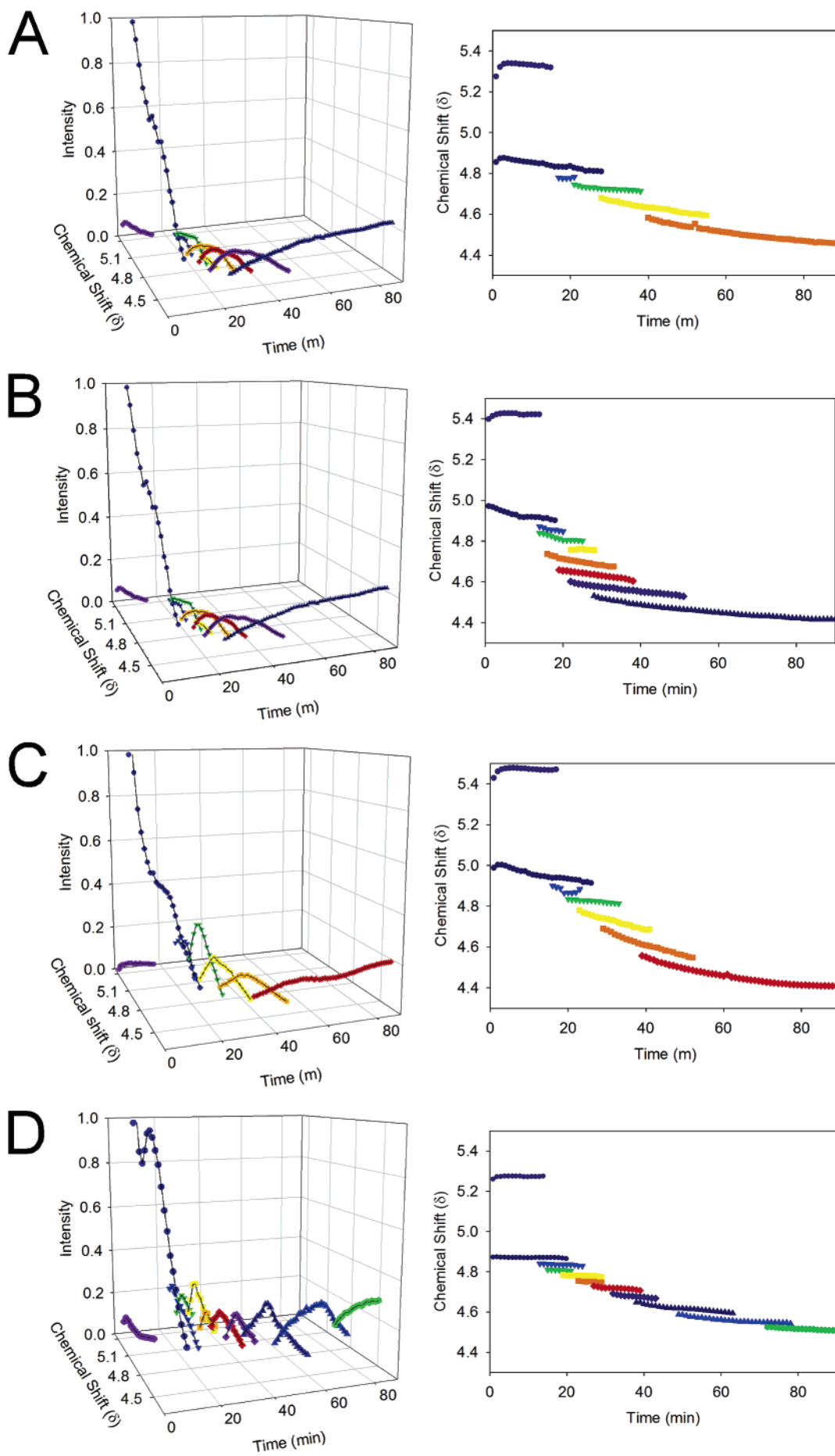
**Water Structure Probed Using Solution NMR.** Reverse micelle water loading (particle size) is distributed according to a Poisson distribution, with a spherical water core and low polydispersity.<sup>43–46</sup> Near room temperature, reverse micelles interact with one another on a time scale of microseconds to milliseconds.<sup>44,45</sup> Translational diffusion measurements derived from pulsed-field gradient diffusion NMR experiments have a nominal time scale of  $\sim 100$  ms and indicate that the average

(43) Zulauf, M.; Eicke, H. F. *J. Phys. Chem.* **1979**, *83*, 480–486.

(44) Clark, S.; Fletcher, P. D. I.; Ye, X. *Langmuir* **1990**, *6*, 1301–1309.

(45) Jain, T. K.; Cassin, G.; Badiali, J. P.; Pileni, M. P. *Langmuir* **1996**, *12*, 2408–2411.

(46) Politi, M. J.; Chaimovich, H. *J. Phys. Chem.* **1986**, *90*, 282–287.



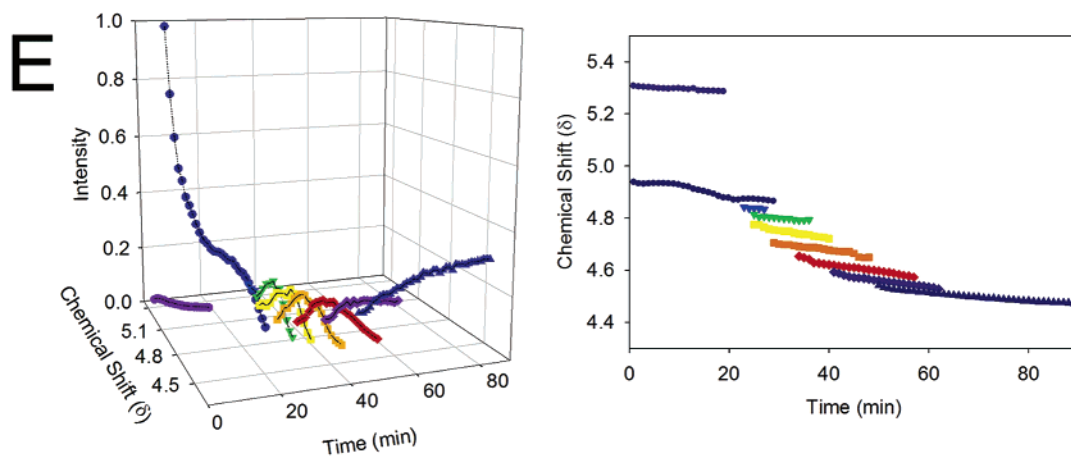


**Figure 6.** Water resonance intensity and chemical shift versus time at low temperature. The plots demonstrate changes from the presence of multiple populations of water that coexist for several minutes (macroscopic time scale). (A–C) are 1 M, 500 mM, and 250 mM NaCl at  $-30\text{ }^{\circ}\text{C}$ , respectively. (D and E) are 500 mM and 250 mM NaCl at  $-20\text{ }^{\circ}\text{C}$ , respectively.

**Table 2.** Number of Populations of Water at Different Temperatures and Salt Concentrations

temp, $^{\circ}\text{C}$	1 M NaCl populations	0.5 M NaCl populations	0.25 M NaCl populations
$-30$	6	9	7
$-20$	1	9	9

reverse micelle radii at room temperature are very close to the values predicted based on formulation.<sup>47</sup> Photon correlation spectroscopy has been used to determine the size and shape of aggregates; water present in the reverse micelles promote a spherical shape.<sup>16,43</sup> Results included here confirm the presence of several distinct chemical shifts for the water resonance that are persistent for several minutes. These data do not unambiguously indicate whether the distinct coincident water environments lie within a single reverse micelle particle or whether a distribution of environments is reflected. Some averaging of water molecules remains possible, but as water loading decreases, the polydispersity of the reverse micelles decreases, and therefore the changes in chemical shifts most likely correspond to multiple and distinct populations of water within individual micelles.

Careful measurement of the time dependence of the water chemical shift allows us to monitor time-dependent changes in the structure of water. The  $^1\text{H}$  chemical shift dependence of encapsulated water on  $w_0$  at  $25\text{ }^{\circ}\text{C}$  has been previously investigated and is well-fit by a single-exponential function, which results in a simple expression in  $w_0$ :  $\delta(w_0) = 4.0249 + 0.8979(1 - e^{-0.0766w_0})$ ; e.g., the  $^1\text{H}$  chemical shift of the water resonance has an exponential dependence on  $w_0$ .<sup>22,24</sup> Nowak and co-workers have determined that, within the limit of low water loading conditions, e.g.,  $<10$ , most of the water molecules will be involved in solvation of the surfactant headgroup or counterions, leaving relatively few molecules to participate in hydrogen bonding.<sup>22,23</sup> At low  $w_0$ , ion–dipole interactions between the surfactant headgroup and water molecules restrict the motion of the water molecules, producing relatively long residence times, e.g., long correlation times.<sup>22,48</sup> As the water loading increases and the surfactant headgroups become com-

pletely solvated, water not involved in the solvation shell adopts an optimized hydrogen bonding geometry resulting in an accompanying downfield shift. Water loading values above 6 have been reported to lead to the formation of a limiting water pool, and the lifetime of the water in both the solvated shell and the water pool is about  $10^{-4}\text{ s}^{-1}$ .<sup>22,23</sup> As more and more water is added to the system, this hydrogen bonding geometry is further optimized, with water in the reverse micelle finally ending with a hydrogen bonding geometry of bulklike water at a  $w_0$  of 40.<sup>23</sup>

Water in biological systems is confined within a cell, often trapped between membranes in the organelles. The motion of water is also restricted at or near the surface of proteins; examples include water ordered around the charged outer surface of a protein or water confined to cavities within a protein or transient cavities involved in enzyme/substrate turnover. These water molecules will have different physical properties than those of bulk water. The salient physical feature of bulk water is the hydrogen bonding networks formed within it, between water molecules as well as between water and the hydrogen bond donors and acceptors of solute molecules. The structure of water confined within reverse micelles is significantly influenced by interactions with the surfactant headgroups and associated counterions, and in this sense, encapsulated water is similar to that found confined within cellular compartments or associated with biological macromolecules. Water confined within a reverse micelle can provide crucial clues to the study of confined or restricted water, since low-temperature studies indicate that ionic strength can be used to tune the reverse micelles to water pools of various sizes.

**Biophysical Studies of Proteins.** In much the same way that cellular water is confined, proteins in the cells are crowded by other substrates or compartmentalized within a cell membrane. Proteins in confined spaces have been shown to have energetics that are distinct from their counterparts in bulk solution due to a restriction on conformational entropy.<sup>49,50</sup> Reverse micelles provide an effective model for the confined environment necessary to study the energetics of conformationally restricted proteins. The phenomenon of water shedding can serve as a

(47) Wand, A. J.; Flynn, P. F.; Ehrhardt, M. R. *Proc. Natl. Acad. Sci.* **1998**, *95*, 15299–15302.

(48) Riter, R. E.; Undiks, E. P.; Levinger, N. E. *J. Am. Chem. Soc.* **1998**, *120*, 6062–6067.

(49) Eggers, D. K.; Valentine, J. S. *Protein Sci.* **2001**, *10*, 250–261.

(50) Zhou, H. X.; Dill, K. A. *Biochemistry* **2001**, *40*, 11289–11293.



fine-tuning method, allowing the precise dimensions of the reverse micelle to be readily adjusted.

**Supercooled Water.** Previous studies have established that a supercooled state of water may be generated using thin films, capillary samples, droplet samples, and emulsions, e.g., under conditions that minimize homogeneous nucleation, and our results confirm that water under such conditions may be supercooled to at least  $-39.5\text{ }^{\circ}\text{C}$  at 1 atm of pressure, although literature values report reverse micelles that at very low  $w_0$  values remain stable at even lower temperatures.<sup>21,51,52</sup> Reverse micelles thus provide an excellent alternative approach to studies of supercooled water, since they support investigation of water structure without the use of high external pressures or the addition of other solvents, such as ethyl alcohol or glycerol. There is significant controversy regarding exact physical description of the structure of supercooled water, but there is general agreement that with decreasing temperature the hydrogen bonding interactions among the water molecules are optimized, leading to the four-coordinate geometry of ice, which creates an open network character.<sup>34,51</sup> As previously mentioned, we note the existence of multiple and distinct populations of water and observe that reverse micelles are an excellent vehicle for examining distinct populations of supercooled water (see Figure 6). The ability to directly observe multiple coexisting populations of water represents an important new approach for the study of the structure of supercooled water.

**Influence of Ionic Strength.** Results presented here confirm that reverse micelles reconstituted from solutions of high ionic strength have a higher water loading capacity than low ionic strength reverse micelles at low temperatures. Previous studies have suggested that at low temperature the average radii of reverse micelles decrease with increasing ionic strength, but the studies did not focus on the details of the water shedding process.<sup>21,25,26</sup> Based on the available thermodynamic considerations, the observed increased water holding capacity of such reverse micelle preparations is most probably due to an increase in the heat capacity of a supercooled water pool. The high relative heat capacity of supercooled water is in turn generally considered to originate from the long range order of water molecules produced by cooperative interactions among the structural elements of the liquid.<sup>53</sup> It can therefore be inferred that the structural ordering of water at low temperatures has a substantial influence on the heat capacity of the water which in turn affects the enthalpy of the reverse micelle system at low temperatures. The general dependence of the free energy of the system on the change in heat capacity is described in the following expression.<sup>54</sup>

$$\Delta G(T_f) = \Delta H(T_i) + \Delta C_p(T_f - T_i) - T_f(\Delta S(T_i) + \Delta C_p \ln(T_f/T_i)) \quad (1)$$

wherein  $T_i$  and  $T_f$  represent initial and final temperatures, respectively;  $\Delta H$ ,  $\Delta S$ , and  $\Delta G$  are the change in molar enthalpy, entropy and free energy respectively; and  $\Delta C_p$  is the molar change in the heat capacity at constant pressure.

According to the prevailing theory, encapsulation of water with reverse micelles leads to a positive increase in system enthalpy.<sup>55</sup> Given that encapsulation is a spontaneous process, the positive change in enthalpy must necessarily be compensated by a net positive change in the system entropy ( $-T\Delta S$ ).<sup>55-57</sup> Thus, as the temperature of the system is lowered, the encapsulated water begins to supercool, and as the temperature continues to decrease past a critical transition temperature, entropy will dominate the system and the reverse micelles will expel water until equilibrium is established within the system. The most direct interpretation of our results is that reconstitution of reverse micelles from buffers of relatively high ionic strength leads to an increase in the heat capacity for the encapsulation process, which in turn stabilizes higher  $w_0$  at lower temperatures.

Another aspect of ionic strength is its corresponding effect on the hydrogen bonding properties of water. The hydrogen bond is composed of covalent and electrostatic components. Increasing the covalency would decrease the strength of the hydrogen bond as this decreases the length of the bond; increasing the length of a hydrogen bond therefore corresponds to an increase in its electrostatic component. Thus, ions will affect the length of the hydrogen bonds and therefore the structure of a hydrogen bonding network. Jones and Dole investigated the viscosities of aqueous solutions as a function of their ion concentration and found the following relation:  $\eta = \eta_0(1 + A\sqrt{c} + Bc)$  where  $\eta$  is the viscosity and  $c$  is the relative ion concentration.<sup>52</sup> The  $B$  term represents the effect ions have on the hydrogen bonding of water, and this in turn will affect the viscosity of a solution. The Jones–Dole  $B$  term is important at high ion concentrations, as would be seen in a reverse micelle of high ionic strength, and the sign of the variable indicates whether the ions will be kosmotropes, structure inducing ions, or chaotropes, structure breaking ions. In the case of  $\text{Na}^+$ ,  $\text{Cl}^-$ , and the sulfonate group, the  $B$  term is positive, indicating that the ions function as kosmotropes.<sup>58-61</sup>

**Rigidity and Reverse Micelle Behavior.** In addition to its influence over the physiochemical behavior over water, ionic strength affects the flexibility of the surfactant aggregate by interacting with the anionic headgroups of the AOT.<sup>62,63</sup> Work by several groups generates a portrait of the interior surface of reverse micelles which invokes a network of AOT headgroups with a closely associated network of interacting ions and water molecules.<sup>62,63</sup> It is generally accepted that, at ambient temperatures, increasing amounts of salt reduces the radii of the micelles, suggesting that the surfactant molecules pack more densely. Our results show a correlation between ionic strength and low-temperature reverse micelle stability that suggests that the ionic-strength-induced rigidity is a fundamental aspect of low-temperature reverse micelle stability.

**Water Shedding.** Recently, the conductance of encapsulated water shed from AOT reverse micelles reconstituted from water solutions of high ionic strength was examined in detail.<sup>20</sup> Following incubation of the system at  $-20\text{ }^{\circ}\text{C}$ , the conductance

(51) Angell, C. A. *Annu. Rev. Phys. Chem.* **1983**, *34*, 593–630.

(52) Dill, K. A.; Bromberg, S. *Molecular Driving Forces: Statistical Thermodynamics in Chemistry and Biology*; Garland Science: New York, 2003.

(53) Oguni, M.; Angell, C. A. *J. Chem. Phys.* **1983**, *78*, 7334–7342.

(54) Fersht, A. *Structure and Mechanism in Protein Science: A Guide to Enzyme Catalysis and Protein Folding*; W. H. Freeman and Company: New York, 1998.

(55) Moulik, S. P.; Bhattacharya, P. K. *Langmuir* **1992**, *8*, 2135–2139.

(56) D'Aprano, A.; Lizzio, A.; Liveri, V. T. *J. Phys. Chem.* **1987**, *91*, 4749–4751.

(57) Ray, S.; Moulik, S. P. *Pure Appl. Chem.* **1994**, *66*, 521–525.

(58) Tsierkezos, N. G.; Molinou, I. E. *Z. Phys. Chem.* **2004**, *218*, 211–217.

(59) Jones, G.; Talley, S. *J. Am. Chem. Soc.* **1933**, *55*, 624.

(60) Jones, G.; Stauffer, R. E. *J. Am. Chem. Soc.* **1940**, *62*, 336.

(61) Laurence, V. D.; Wolfenden, J. H. *J. Chem. Soc.* **1934**, 1144.

(62) Leodidis, E. B.; Hatton, T. A. *Langmuir* **1989**, *5*, 741–753.

(63) Bardez, E.; Vy, N. C. *Langmuir* **1995**, *11*, 3374–3381.

of water shed from reverse micelles composed of a 1.5 M solution of NaCl was found to be equivalent to  $\sim 270$  nM NaCl solution. This represents a decrease in salt concentration of the liberated water of approximately 4 orders of magnitude, as salt and probe molecules remain confined within the reverse micelle. The ability of reverse micelles to separate the water and salt from the water pool suggests a host of future applications, including both water purification schemes and nanoparticle formation.<sup>7</sup> This observation revises the conclusions of previous studies that under the influence of low-temperature perturbation

the reverse micelle system sheds water, salt, and surfactant at low temperatures.<sup>21</sup>

**Acknowledgment.** The research was supported by a Seed Grant Award from the University of Utah Research Foundation and an NIH Training Grant GM8537 (A.K.S and W.V.H.). The authors thank Amy C. Spencer for critical reading of the manuscript.

JA0568401